

The Pre-Reactive Complex of H₂S and BrCl; Observation and Characterisation by Rotational Spectroscopy

Hannelore I. Bloemink and A. C. Legon*

Abstract: By using a fast-mixing nozzle in a Fourier transform microwave spectrometer, any chemical reaction accompanying mixing of H₂S and BrCl was prevented, thus allowing the observation of the pre-reactive complex H₂S...BrCl. The rotational spectra of eight isotopomers of the complex were recorded. The analysis of the determined spectroscopic constants shows that the atoms S...Br-Cl are

collinear or nearly so and that the H₂S plane is approximately perpendicular to the S...Br-Cl axis with $r(\text{S}\cdots\text{Br}) =$

3.094(7) Å. This geometry is in agreement with previously stated rules for B...XY complexes, where B is a Lewis base and XY is an (inter)halogen molecule. The intermolecular interaction is shown to be relatively weak, both in terms of the intermolecular stretching force constant k_s and the intramolecular electric charge redistribution δ within the BrCl subunit that accompanies formation of H₂S...BrCl.

Keywords

cyclic compounds · medium-sized rings · tetraketones · transannular interactions

1. Introduction

A number of pre-reactive complexes B...XY, where B is a Lewis base and XY is an (inter)halogen, have been investigated recently.^[1,2] One of the aims of these studies is to determine whether there is any significant extent of electric charge transfer between the two molecules when the complex is formed from its components. In the language of Mulliken^[3] the question of interest is whether the complex is of the "inner" [BX]⁺...Y⁻ (strong binding, significant intermolecular charge transfer) or the "outer" B...XY (weak binding, minor intermolecular charge transfer) type. An additional aim is to examine whether rules^[4] for predicting the angular geometries of the hydrogen-bonded complexes B...HX also apply to B...XY complexes.

A detailed characterisation of the complex formed by H₂S and BrCl represents an important objective in achieving these aims for two reasons. First, it is generally accepted^[5] that the order of electron-acceptor ability among halogen or interhalogen molecules in forming complexes B...XY is ICl > BrCl > I₂ > Br₂ > Cl₂, and hence BrCl is expected to lead to strong complexes and to enhance the possibility of charge transfer when involved in a complex with a given Lewis base B. Second, the hydrogen bonded H₂S...HX complexes have a right-angled structure, that is, the H₂S plane is approximately perpendicular to the S...X axis,^[6] a result that can be understood according to the rules if the HX axis is assumed to lie along the axis of a nonbonding electron pair carried by S. Such a structure for H₂S...BrCl would be a strong indication that the rules also apply to B...XY complexes.

In this paper we report the observation and characterisation of a complex formed between H₂S and BrCl. This was achieved by using a Fourier-transform microwave spectrometer, fitted with a fast-mixing nozzle^[7] to prevent any chemical reaction between the two species. The results are analysed in terms of geometry of the complex and electric charge redistribution within BrCl upon complex formation and are compared with those for a number of related complexes.

2. Results

2.1. Spectral analysis: The observed spectrum of each of the isotopomers was that of a nearly prolate asymmetric-top molecule with a large rotational constant A_0 and exhibited hyperfine structure characteristic of the presence of the two nuclei Br ($I = 3/2$) and Cl ($I = 3/2$) on or close to the a axis of the complex. Frequencies of the observed transitions for the isotopomers H₂S...⁷⁹Br³⁵Cl, H₂S...⁸¹Br³⁵Cl, H₂S...⁷⁹Br³⁷Cl, H₂S...⁸¹Br³⁷Cl, HDS...⁷⁹Br³⁵Cl, HDS...⁸¹Br³⁵Cl, D₂S...⁷⁹Br³⁵Cl and D₂S...⁸¹Br³⁵Cl can be found in Tables 1–4. When the complex geometry established in Section 2.2 is used, the predicted rotational constants for the isotopomer H₂S...⁷⁹Br³⁵Cl are $A = 141082.5$ MHz, $B = 1053.5502$ MHz and $C = 1053.0304$ MHz, leading to a Ray's asymmetry parameter $\kappa = -0.999992$. As might be expected, a -type transitions having $K_{-1} \geq 0$ were not observed since these levels lie ≥ 4.7 cm⁻¹ in wave number above the $K_{-1} = 0$ levels and are thus rotationally cooled in the supersonic expansion. The established geometry also implies a nonzero value of the c component of the electric dipole moment but transitions allowed by μ_c were predicted to lie outside the frequency range of our spectrometer. Hence, the observed spectrum consisted only of the μ_a transitions $(J+1)_{0,J+1} \leftarrow J_{0,J}$.

[*] Prof. Dr. A. C. Legon and Dr. H. I. Bloemink
Department of Chemistry, University of Exeter
Stocker Road, Exeter EX44QD (UK)
Fax: Int. code + (1392) 263-434
e-mail: ACLegon@exeter.ac.uk

When κ is so close to -1 , the observed $(J+1)_{0,J+1} \leftarrow J_{0,J}$ transition frequencies of the complex can be fitted by using a Hamiltonian for a $K=0$ symmetric-top molecule.^[8] The Hamiltonian operator H used is given by Equation (1), where H_R is the rotational energy operator [Eq. (2)], $H_{Q(X)}$ is the

$$H = H_R + H_{Q(\text{Br})} + H_{Q(\text{Cl})} + H_{\text{SR}(\text{Br})} + H_{\text{SR}(\text{Cl})} \quad (1)$$

$$H_R = \frac{1}{2}(B_0 + C_0)J^2 - D_J J^4 \quad (2)$$

energy operator describing the interaction of the electric quadrupole moment $Q(X)$ ($X = \text{Br}$ or Cl) with the electric field gradient $\nabla E(X)$ at the appropriate nucleus [Eq. (3)], and

$$H_{Q(X)} = -\frac{1}{6}Q(X) : \nabla E(X) \quad (3)$$

$H_{\text{SR}(X)}$ is the energy operator describing the interaction of the magnetic dipole moment $\mu(X) = g(X)\mu_N I(X)$ with the magnetic field strength $B(X)$ at X resulting from the molecular rotation [Eq. (4)], where $M(X)$ is the spin-rotation coupling tensor of

$$H_{\text{SR}(X)} = -I(X) \cdot M(X) \cdot J \quad (4)$$

the nucleus X . The Hamiltonian H was set up in the coupled basis $I(\text{Br}) + I(\text{Cl}) = I$, $I + J = F$ and was diagonalised in blocks of F . The matrix elements of $H_{Q(X)}$ and $H_{\text{SR}(X)}$ in this basis have been given elsewhere.^[9, 10] The assignment of the observed transitions using labels and quantum numbers appropriate to this basis can be found in Tables 1–4. The spectroscopic constants determined in the least-squares fit of transi-

Table 1. Observed and calculated transition frequencies of $\text{H}_2\text{S} \cdots {}^{79}\text{Br}^{35}\text{Cl}$ and $\text{H}_2\text{S} \cdots {}^{81}\text{Br}^{35}\text{Cl}$.

$J' \leftarrow J''$	I'	$F' \leftarrow F''$	$\text{H}_2\text{S} \cdots {}^{79}\text{Br}^{35}\text{Cl}$		$\text{H}_2\text{S} \cdots {}^{81}\text{Br}^{35}\text{Cl}$	
			$\nu_{\text{obs}}/\text{MHz}$	$\Delta\nu/\text{kHz}$ [a]	$\nu_{\text{obs}}/\text{MHz}$	$\Delta\nu/\text{kHz}$ [a]
$4_{04} \leftarrow 3_{03}$	0	4 \leftarrow 0	8417.4525	0.1	8417.3298	-1.3
	1	5 \leftarrow 1	8418.1225	-0.2	8418.1020	1.7
	2	5 \leftarrow 2	8418.9238	-0.7	8418.7930	-1.1
	1	4 \leftarrow 1	8419.8583	2.2	8419.7469	-2.6
	2	6 \leftarrow 2	8419.8810	0.9	8419.7469	1.5
	3	7 \leftarrow 3	8420.6516	0.8	8420.5091	1.4
	1	3 \leftarrow 1	8420.6782	-2.2	8420.5722	-0.9
	3	6 \leftarrow 3	8421.1679	-1.2	8421.0931	-0.6
	3	2 \leftarrow 3	—	—	8435.0607	-0.4
	3	4 \leftarrow 3	8440.9873	0.4	8437.1993	1.1
	3	3 \leftarrow 2	8441.1485	-1.5	8437.3536	0.5
	2	3 \leftarrow 2	8443.2208	0.4	8439.0617	0.2
	3	5 \leftarrow 3	8445.8237	0.0	8441.9396	0.2
	2	4 \leftarrow 2	8447.4676	1.0	8443.2653	0.3
	0	5 \leftarrow 0	10526.7425	-0.1	10526.0417	0.0
	1	6 \leftarrow 1	10527.4904	-1.5	10526.8638	0.8
$5_{05} \leftarrow 4_{04}$	2	6 \leftarrow 2	10527.6082	0.7	10526.8929	-1.1
	1	5 \leftarrow 1	10528.1571	0.4	10527.4622	2.6
	2	7 \leftarrow 2	10528.3620	-2.6	10527.6498	-3.5
	1	4 \leftarrow 1	10528.3805	6.0	10527.6747	4.5
	3	8 \leftarrow 3	10528.8066	-1.2	10528.0914	0.5
	3	7 \leftarrow 3	10529.1026	0.3	10528.4228	-0.8
	0	5 \leftarrow 1	10531.8930	-1.3	—	—
	3	3 \leftarrow 2	10540.2887	0.1	10537.2471	-0.6
	3	4 \leftarrow 3	10540.8016	-1.5	10537.9285	-0.3
	3	5 \leftarrow 3	10541.3380	1.8	10538.4356	-0.9
	3	2 \leftarrow 3	10541.9318	-0.1	—	—
	2	4 \leftarrow 2	10542.6001	-1.1	10539.5548	0.9
	2	3 \leftarrow 2	10542.9563	-0.8	10540.0230	-1.2
	3	6 \leftarrow 3	10543.7224	0.3	10540.7684	0.7
	2	5 \leftarrow 2	10544.3926	0.6	10541.3380	-1.6

[a] $\Delta\nu = \nu_{\text{obs}} - \nu_{\text{calcd}}$.

Table 2. Observed and calculated transition frequencies of $\text{H}_2\text{S} \cdots {}^{79}\text{Br}^{37}\text{Cl}$ and $\text{H}_2\text{S} \cdots {}^{81}\text{Br}^{37}\text{Cl}$.

$J' \leftarrow J''$	I'	$F' \leftarrow F''$	$\text{H}_2\text{S} \cdots {}^{79}\text{Br}^{37}\text{Cl}$		$\text{H}_2\text{S} \cdots {}^{81}\text{Br}^{37}\text{Cl}$	
			$\nu_{\text{obs}}/\text{MHz}$	$\Delta\nu/\text{kHz}$ [a]	$\nu_{\text{obs}}/\text{MHz}$	$\Delta\nu/\text{kHz}$ [a]
$4_{04} \leftarrow 3_{03}$	0	4 \leftarrow 0	8230.3397	0.4	8230.6583	-0.4
	1	5 \leftarrow 1	8230.7908	-0.9	8231.1618	-0.9
	2	5 \leftarrow 2	8231.5049	-0.8	8231.7855	-1.0
	1	4 \leftarrow 1	8232.2241	1.8	8232.5174	-1.5
	2	6 \leftarrow 2	8232.2564	-1.9	8232.5369	0.7
	3	7 \leftarrow 3	8232.8770	1.0	8233.1490	0.1
	1	3 \leftarrow 1	8232.8770	-0.5	8233.2095	1.3
	3	6 \leftarrow 3	8233.2307	0.8	8233.5775	0.2
	3	4 \leftarrow 3	—	—	8250.5423	0.6
	3	5 \leftarrow 3	—	—	8254.3457	0.9
	0	5 \leftarrow 0	10292.5310	0.3	10292.3660	-0.7
	1	6 \leftarrow 1	10293.0725	-0.7	10292.9422	1.1
	2	6 \leftarrow 2	10293.2238	1.2	10293.0305	-1.4
	1	5 \leftarrow 1	—	—	10293.4618	-1.2
	2	7 \leftarrow 2	10293.8128	-2.9	10293.6280	1.9
	1	4 \leftarrow 1	—	—	10293.6605	2.2
$5_{05} \leftarrow 4_{04}$	3	8 \leftarrow 3	10294.1716	0.1	10293.9780	-0.3
	3	7 \leftarrow 3	10294.3740	2.0	10294.2221	0.9
	3	3 \leftarrow 2	10306.3002	-0.2	10303.7788	1.3
	3	4 \leftarrow 3	10306.5735	-1.3	10304.2194	-0.9
	3	5 \leftarrow 3	10307.0254	3.4	10304.6528	0.3
	3	6 \leftarrow 3	10308.9275	-0.2	10306.5339	-0.1
	2	5 \leftarrow 2	10309.5405	-1.5	10307.0075	-3.1

[a] $\Delta\nu = \nu_{\text{obs}} - \nu_{\text{calcd}}$.

Table 3. Observed and calculated transition frequencies of $\text{HDS} \cdots {}^{79}\text{Br}^{35}\text{Cl}$ and $\text{HDS} \cdots {}^{81}\text{Br}^{35}\text{Cl}$.

$J' \leftarrow J''$	I'	$F' \leftarrow F''$	$\text{HDS} \cdots {}^{79}\text{Br}^{35}\text{Cl}$		$\text{HDS} \cdots {}^{81}\text{Br}^{35}\text{Cl}$	
			$\nu_{\text{obs}}/\text{MHz}$	$\Delta\nu/\text{kHz}$ [a]	$\nu_{\text{obs}}/\text{MHz}$	$\Delta\nu/\text{kHz}$ [a]
$4_{04} \leftarrow 3_{03}$	1	5 \leftarrow 1	8267.4997	-0.3	8267.2637	0.4
	2	5 \leftarrow 2	8268.3081	1.2	8267.9567	-0.5
	1	4 \leftarrow 1	8269.2380	0.6	—	—
	2	6 \leftarrow 2	8269.2592	-2.3	8268.9074	-0.6
	3	7 \leftarrow 3	8270.0311	0.4	8269.6691	-0.2
	3	6 \leftarrow 3	8270.5430	0.2	—	—
	3	5 \leftarrow 3	8295.1687	0.0	8291.0752	1.3
	2	4 \leftarrow 2	8296.8334	0.2	8292.4156	-0.5
	0	5 \leftarrow 0	10338.4654	0.0	10337.4925	-1.1
	1	6 \leftarrow 1	10339.2137	0.4	10338.3162	2.1
	2	6 \leftarrow 2	10339.3310	-1.8	10338.3440	-0.7
	1	5 \leftarrow 1	—	—	10338.9105	1.3
	2	7 \leftarrow 2	10340.0898	1.0	10339.1018	-1.7
	3	8 \leftarrow 3	10340.5311	0.0	10339.5404	-0.2
	3	7 \leftarrow 3	10340.8224	0.7	10339.8742	1.4
	3	5 \leftarrow 3	10353.0411	0.7	10349.8743	0.5
$5_{05} \leftarrow 4_{04}$	3	6 \leftarrow 3	10355.4247	-0.1	10352.2033	0.2
	2	5 \leftarrow 2	10356.1019	-0.9	10352.7810	-1.9

[a] $\Delta\nu = \nu_{\text{obs}} - \nu_{\text{calcd}}$.

tion frequencies using the Hamiltonian of Equation (1) are $\frac{1}{2}(B_0 + C_0)$, D_J , $\chi_{aa}(\text{Br})$, $\chi_{aa}(\text{Cl})$, $M_{bb}(\text{Br})$ and $M_{bb}(\text{Cl})$, where $\chi_{aa}(X) = -(eQ(X)/h)(\partial^2 V/\partial a^2)_X$, and their values from the final cycle of the fit are shown in Table 5 for the eight isotopomers investigated. Also included in Table 5 are the standard deviations of the fits, σ . For each isotopomer, σ is smaller than the estimated error in the frequency measurement; this indicates that the Hamiltonian used was adequate, although $M_{bb}(\text{Cl})$ is barely significant.

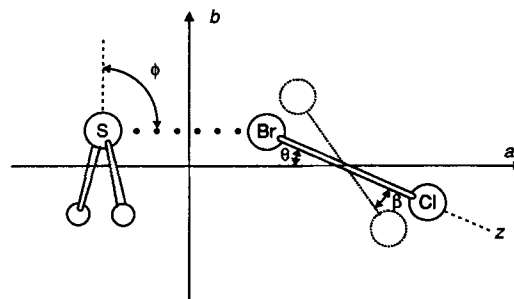
2.2. Structure of the complex: The observed changes in $(B_0 + C_0)/2$ upon isotopic substitution (see Table 5) are consistent only with the order $\text{S} \cdots \text{Br}-\text{Cl}$ of the heavy atoms. The small deviations of $\chi_{aa}(\text{Br})$ and $\chi_{aa}(\text{Cl})$ from the free BrCl values imply that the heavy atoms are collinear or nearly so, a result

Table 4. Observed and calculated transition frequencies of $D_2S \cdots {}^{79}Br^{35}Cl$ and $D_2S \cdots {}^{81}Br^{35}Cl$.

$J' \leftarrow J''$	I'	$F' \leftarrow F''$	$D_2S \cdots ^{79}Br^{35}Cl$		$D_2S \cdots ^{81}Br^{35}Cl$		
			$\nu_{\text{obs}}/\text{MHz}$	$\Delta\nu/\text{kHz}$ [a]	$\nu_{\text{obs}}/\text{MHz}$	$\Delta\nu/\text{kHz}$ [a]	
$4_{04} \leftarrow 3_{03}$	0	$4 \leftarrow 0$	3	8123.6850	0.1	—	—
	1	$5 \leftarrow 1$	4	8124.3520	0.3	8123.8904	−1.6
	2	$5 \leftarrow 2$	4	8125.1597	−0.9	8124.5878	−1.3
	1	$4 \leftarrow 1$	3	8126.0892	1.3	—	—
	2	$6 \leftarrow 2$	5	8126.1116	−1.9	8125.5378	−0.4
	3	$7 \leftarrow 3$	6	8126.8794	−1.3	8126.2971	−0.2
	3	$6 \leftarrow 3$	5	8127.3887	1.7	8126.8794	2.4
	3	$4 \leftarrow 3$	3	8147.1563	0.0	—	—
	3	$5 \leftarrow 3$	4	8151.9847	1.5	8147.6786	0.5
	2	$4 \leftarrow 2$	3	8153.6685	−0.8	8149.0356	0.6
$5_{05} \leftarrow 4_{04}$	0	$5 \leftarrow 0$	4	10159.5309	0.0	10158.2845	1.2
	1	$6 \leftarrow 1$	5	10160.2772	0.6	10159.1033	1.9
	2	$6 \leftarrow 2$	5	10160.3980	0.1	10159.1339	−1.0
	1	$5 \leftarrow 1$	4	10160.9439	−0.8	10159.6996	0.5
	2	$7 \leftarrow 2$	6	10161.1533	0.9	10159.8903	−1.6
	3	$8 \leftarrow 3$	7	10161.5942	0.5	10160.3284	0.9
	3	$7 \leftarrow 3$	6	10161.8809	−0.3	10160.6571	−0.3
	3	$4 \leftarrow 3$	3	10173.5596	1.9	10170.1462	1.2
	3	$5 \leftarrow 3$	4	10174.0868	−0.9	10170.6507	0.8
	2	$4 \leftarrow 2$	3	10175.3671	−0.9	10171.7790	−0.7
	2	$3 \leftarrow 2$	2	10175.7059	−0.6	—	—
	3	$6 \leftarrow 3$	5	10176.4675	0.0	10172.9762	−0.3
	2	$5 \leftarrow 2$	4	10177.1541	−0.4	10173.5596	−2.6

[a] $\Delta\nu = \nu_{obs} - \nu_{calc}$.

established in detail in Section 2.3. In the model used to determine the geometry of the complex, the monomer geometries (Table 6)^[11, 12] are assumed to be unchanged upon complex formation; thence only the angles θ and ϕ and the distance $r(S \cdots Br)$ defined in Figure 1 are required. By keeping the angle θ fixed at 0° (as dictated by the conclusion of Section 2.3), a value of the bond length $r(S \cdots Br)$ for each angle ϕ can be

Fig. 1. Definition of the angles ϕ and θ and the distance $r(S \cdots Br)$ used in the discussion of the complex geometry. The principal inertial axes a and b are also indicated.

calculated by fitting the observed value ($B_0 + C_0$) for the isotopomer $H_2S \cdots {}^{79}Br^{35}Cl$ (the parent complex). In this way, pairs of $r(S \cdots Br)$ and ϕ values that reproduce ($B_0 + C_0$) are established. For each pair of quantities, ($B + C$) is calculated for the deuterated isotopomers $D_2S \cdots {}^{79}Br^{35}Cl$ and $HDS \cdots {}^{79}Br^{35}Cl$, so that the difference $\Delta(B + C)$ in ($B + C$) between the parent complex and each of the deuterated complexes can then be obtained as a function of the angle ϕ ; this results in the curves shown in Figure 2. The observed values of $\Delta(B_0 + C_0)$ are indicated by the solid lines and lead to $\phi = 96.1(13)^\circ$ and $r(S \cdots Br) = 3.094(6) \text{ \AA}$ when the isotopomer $D_2S \cdots BrCl$ is used and $\phi = 95.9(13)^\circ$ and $r(S \cdots Br) = 3.094(7) \text{ \AA}$ for the $HDS \cdots BrCl$ isotopomer. With the average value of $\phi = 96.0(13)^\circ$ (and thus $r(S \cdots Br) = 3.094(7) \text{ \AA}$), the difference between the observed and calculated ($B + C$)/2 for all investigated isotopomers are as shown in Table 7. The errors in ϕ and $r(S \cdots Br)$ were estimated by assuming a deviation of $\pm 10^\circ$ of the $S \cdots Br-Cl$ nuclei from collinearity (see Section 2.3).

Table 5. Ground-state spectroscopic constants of eight isotopomers of $H_2S \cdots BrCl$.

	$1/2(B_0 + C_0)/MHz$	D_J/kHz	$\chi_{aa}(Br)/MHz$	$\chi_{aa}(Cl)/MHz$	$M_{ab}(Br)/kHz$	$M_{ab}(Cl)/kHz$	σ/kHz [c]
$H_2S \cdots {}^{79}Br^{35}Cl$	1053.2903 (1)	0.503 (3)	885.96 (4)	−93.78 (1)	−3.3 (3)	−0.1 (1)	1.7
$H_2S \cdots {}^{81}Br^{35}Cl$	1053.1513 (1)	0.504 (2)	740.14 (3)	−93.78 (1)	−3.8 (3)	0.0 (2)	1.7
			885.98 (4) [a]				
$H_2S \cdots {}^{79}Br^{37}Cl$	1029.8354 (1)	0.483 (3)	886.30 (5)	−73.90 (2)	−4.1 (3)	−0.5 (2)	1.8
				−93.77 (3) [b]			
$H_2S \cdots {}^{81}Br^{37}Cl$	1029.7484 (1)	0.473 (2)	740.32 (3)	−73.92 (1)	−4.2 (3)	−0.1 (1)	1.4
			886.20 (4) [a]	−93.80 (1) [b]			
$HDS \cdots {}^{79}Br^{35}Cl$	1034.4613 (1)	0.487 (1)	885.95 (2)	−93.68 (1)	−4.0 (2)	0.3 (2)	1.1
$HDS \cdots {}^{81}Br^{35}Cl$	1034.2958 (1)	0.499 (2)	739.87 (3)	−93.66 (2)	−2.0 (3)	−0.2 (2)	1.4
			885.66 (4) [a]				
$D_2S \cdots {}^{79}Br^{35}Cl$	1016.5661 (1)	0.466 (2)	885.87 (2)	−93.43 (1)	−3.4 (2)	0.1 (1)	1.1
$D_2S \cdots {}^{81}Br^{35}Cl$	1016.3731 (1)	0.475 (2)	739.84 (3)	−93.53 (2)	−1.8 (3)	0.7 (3)	1.5
			885.62 (4) [a]				

[a] The observed $\chi_{aa}({}^{81}Br)$ multiplied by the ratio $Q({}^{79}Br)/Q({}^{81}Br)$ from ref. [12]. [b] The observed $\chi_{aa}({}^{37}Cl)$ multiplied by the ratio $Q({}^{35}Cl)/Q({}^{37}Cl)$ from ref. [12]. [c] The σ are the standard deviations of the fits reported in Tables 1–4.

Table 6. Spectroscopic and geometric properties of H_2S [a] and $BrCl$ [b].

	A_0/MHz	B_0/MHz	C_0/MHz	$\chi_0(Br)/MHz$	$\chi_0(Cl)/MHz$	Geometry
H_2S	310182.24	270884.05	141705.88			$\angle HSH = 92.13^\circ$
HDS	292351.30	147861.80	96704.12			$r_0(S-H) = 1.3518 \text{ \AA}$
D_2S	164571.12	135380.31	73244.07			
${}^{79}Br^{35}Cl$		4559.3827 (1)		875.309 (1)	−102.450 (2)	$r_0 = 2.138766 \text{ \AA}$ [c]
${}^{81}Br^{35}Cl$		4524.8598 (1)		731.223 (1)	−102.451 (2)	
${}^{79}Br^{37}Cl$		4388.9109 (1)		875.304 (1)	−80.740 (2)	
${}^{81}Br^{37}Cl$		4354.3855 (1)		731.219 (1)	−80.740 (2)	

[a] Ref. [11]. [b] Ref. [12]. [c] Calculated from the rotational constants.

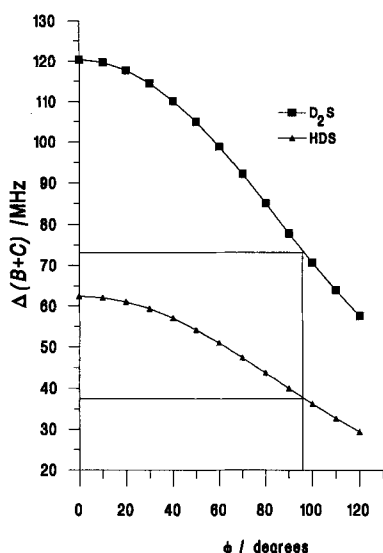


Fig. 2. The calculated difference $\Delta(B+C)$ in $(B+C)$ between $\text{H}_2\text{S} \cdots {}^{79}\text{Br}^{35}\text{Cl}$ and $\text{D}_2\text{S} \cdots {}^{79}\text{Br}^{35}\text{Cl}$ and between $\text{H}_2\text{S} \cdots {}^{79}\text{Br}^{35}\text{Cl}$ and $\text{HDS} \cdots {}^{79}\text{Br}^{35}\text{Cl}$, respectively, as a function of the angle ϕ . The experimental values $\Delta(B_0 + C_0)$ are indicated by the horizontal lines.

Table 7. Observed and calculated values of $1/2(B+C)$ and stretching force constant k_σ for eight isotopomers of $\text{H}_2\text{S} \cdots \text{BrCl}$ [a].

	$1/2(B_0 + C_0)/\text{MHz}$	$1/2(B+C)_{\text{calc}}/\text{MHz}$	k_σ/Nm^{-1}
$\text{H}_2\text{S} \cdots {}^{79}\text{Br}^{35}\text{Cl}$	1053.2903	1053.29	12.17
$\text{H}_2\text{S} \cdots {}^{81}\text{Br}^{35}\text{Cl}$	1053.1513	1053.29	12.15
$\text{H}_2\text{S} \cdots {}^{79}\text{Br}^{37}\text{Cl}$	1029.8354	1030.07	11.84
$\text{H}_2\text{S} \cdots {}^{81}\text{Br}^{37}\text{Cl}$	1029.7484	1029.95	12.10
$\text{HDS} \cdots {}^{79}\text{Br}^{35}\text{Cl}$	1034.4613	1034.47	12.19
$\text{HDS} \cdots {}^{81}\text{Br}^{35}\text{Cl}$	1034.2958	1034.26	11.91
$\text{D}_2\text{S} \cdots {}^{79}\text{Br}^{35}\text{Cl}$	1016.5661	1016.53	11.86
$\text{D}_2\text{S} \cdots {}^{81}\text{Br}^{35}\text{Cl}$	1016.3731	1016.29	12.17

[a] The calculations were done with $\phi = 96.0^\circ$ and $r(\text{S} \cdots \text{Br}) = 3.094 \text{ \AA}$.

The large angle $\phi \approx 96^\circ$ is consistent with a permanently pyramidal configuration at S, with no inversion to the equivalent form with $\phi \approx -96^\circ$ on the timescale of this experiment. As discussed elsewhere^[13] for $\text{H}_2\text{S} \cdots \text{Cl}_2$, the absence of inversion splitting and μ_a transitions involving $K_{-1} > 0$ supports the conclusion that μ_c is nonzero. On the other hand, $K_{-1} = 1$ transitions are observed in related molecules like $\text{H}_3\text{P} \cdots \text{Cl}_2$, in which μ_c is identically zero.^[14]

2.3. Interpretation of the nuclear quadrupole coupling constants:

The nuclear quadrupole coupling constants $\chi_{aa}(\text{Br})$ and $\chi_{aa}(\text{Cl})$ contain information about the electric charge redistribution in the BrCl subunit upon complex formation and the collinearity of the heavy nuclei in the complex. The first obvious conclusion is that the observed values $\chi_{aa}(\text{Br})$ and $\chi_{aa}(\text{Cl})$ do not differ dramatically from the free BrCl molecule values $\chi_0(\text{X})$; the differences are only +1.2% and -8.8%, respectively (see Table 6 for the free-molecule values^[11, 12]).

The small deviation of $\chi_{aa}(\text{Br})$ and $\chi_{aa}(\text{Cl})$ from the free-molecule values can be attributed to three effects. First, there is the change in the electric field gradient (e.f.g.) at the Br or Cl nucleus that arises from the proximity of the electric charge distribution of the H_2S subunit in the complex. As in other $\text{B} \cdots \text{XY}$ complexes (where B is a Lewis base and XY an (inter)halogen) this causes the inner coupling constant $\chi_0(\text{X})$ to increase in absolute value and the outer constant $\chi_0(\text{Y})$ to de-

crease in absolute value relative to the free molecule, to give the modified quantities $\chi'_0(\text{X})$ and $\chi'_0(\text{Y})$, respectively.^[15] Second, the observed $\chi_{aa}(\text{X})$ ($\text{X} = \text{Br}$ or Cl) is the projection of $\chi'_0(\text{X})$ through the angle θ onto the a axis of the complex (see Fig. 1). This effect will decrease both χ 's in absolute value by the factor $P_2(\cos\theta)$. Third, angular oscillation of the BrCl subunit will similarly decrease the magnitude of both χ 's by the factor $\langle P_2(\cos\beta) \rangle$. If there is no variation of the $\chi'_0(\text{X})$ with the angular oscillation of the H_2S subunit, we can derive Equation (5),

$$\chi_{aa}(\text{X}) = \chi'_0(\text{X}) P_2(\cos\theta) \langle P_2(\cos\beta) \rangle \quad (5)$$

where $\text{X} = \text{Br}$ or Cl , $\chi'_0(\text{X})$ is the nuclear quadrupole coupling constant along the BrCl axis z , but changed from the free-molecule value only as a result of the modified e.f.g. at the halogen nucleus X following complex formation and $P_2(\cos\alpha) = 1/2[3\cos^2(\alpha) - 1]$ is the appropriate projection term for the angle $\alpha = \theta$ or β .

The angle θ can be established approximately by considering the effect of dideuteration of the H_2S subunit on the $\chi_{aa}(\text{X})$ values. We can use either $\chi_{aa}({}^{79}\text{Br})$ or $\chi_{aa}({}^{81}\text{Br})$ or $\chi_{aa}({}^{35}\text{Cl})$ for this purpose, since the appropriate values are available (see Table 5). Substitution of H_2S by D_2S causes a rotation of the a axis of the complex through an angle $\delta\theta$. It is a reasonable assumption that this substitution does not affect the angular oscillation of the BrCl subunit, and that $\langle P_2(\cos\beta) \rangle$ therefore remains unchanged. If we further assume that $\chi'_0(\text{X})$ remains unaffected (i.e., there is no change in the e.f.g. along the BrCl axis resulting from D substitution), $\chi(\text{X})$ will change only through the term $P_2(\cos\theta)$ in Equation (5) and hence we can derive Equation (6). The angle $\delta\theta$ can be calculated by using

$$\chi_{aa}(\text{X})_{\text{H}_2\text{S}}/\chi_{aa}(\text{X})_{\text{D}_2\text{S}} = P_2(\cos\theta)/P_2(\cos[\theta + \delta\theta]) \quad (6)$$

the geometry of the complex obtained in Section 2.2, that is, with the $\text{S} \cdots \text{BrCl}$ nuclei collinear. The result is $\delta\theta = 0.591^\circ$ for both $\text{H}_2\text{S} \cdots {}^{79}\text{Br}^{35}\text{Cl}$ and $\text{H}_2\text{S} \cdots {}^{81}\text{Br}^{35}\text{Cl}$ as the parent molecule. Equation (6) leads to $\theta = 0^\circ$ for $\text{X} = {}^{79}\text{Br}$ and $\theta = 0.4^\circ$ for $\text{X} = {}^{81}\text{Br}$ when $\text{H}_2\text{S} \cdots {}^{79}\text{Br}^{35}\text{Cl}$ and $\text{H}_2\text{S} \cdots {}^{81}\text{Br}^{35}\text{Cl}$ are the parent molecules, and to $\theta = 6$ and 4.6° for $\text{X} = {}^{35}\text{Cl}$ when $\text{H}_2\text{S} \cdots {}^{79}\text{Br}^{35}\text{Cl}$ and $\text{H}_2\text{S} \cdots {}^{81}\text{Br}^{35}\text{Cl}$, respectively, are the parent molecule. We conclude that θ is indeed small, in agreement with the requirement $\theta = 0.6^\circ$ when the $\text{S} \cdots \text{BrCl}$ nuclei are collinear. As shown in Section 2.2 a deviation of $\text{S} \cdots \text{BrCl}$ from collinearity by $\pm 10^\circ$ has little effect on the angular geometry derived for $\text{H}_2\text{S} \cdots \text{BrCl}$. We shall assume collinearity in what follows and set $P_2(\cos\theta) \approx 1$.

To calculate $\chi'_0(\text{X})$, a value for the oscillation angle β needs to be estimated. It has been shown^[16] that, for complexes in which an HX subunit is undergoing a two-dimensionally isotropic angular oscillation β , β_{av} scales as $(k_\beta I_b)^{-1/4}$, where I_b is the moment of inertia of the subunit undergoing the oscillation and k_β is the angle bending force constant. Since $k_\sigma = 12.1 \text{ Nm}^{-1}$ for $\text{H}_2\text{S} \cdots \text{BrCl}$ (see Section 2.4) is almost identical to that of the complex $\text{NH}_3 \cdots \text{Cl}_2$ ($k_\sigma = 12.7 \text{ Nm}^{-1}$, $\beta_{\text{av}} = 7.5^\circ$ ^[17]), we assume that k_β is the same for both and hence that the β_{av} will be in the ratio of $I_b^{1/4}$ for Cl_2 and BrCl , leading to $\beta_{\text{av}} = 6.7^\circ$. By using Equation (5), this results in $\chi'_0(\text{Br}) \approx 920 \text{ MHz}$ and $\chi'_0(\text{Cl}) \approx -97 \text{ MHz}$. Indeed, $\chi'_0(\text{X})$ has increased in magnitude for the inner of the halogens (Br) and decreased for the outer one (Cl) compared to their respective free monomer values. For both nuclei, the difference between $\chi'_0(\text{X})$ and $\chi_0(\text{X})$ is approximately 5%, which means that any significant charge redistribution within the BrCl subunit can be ruled out, since this would lead to much larger differences from the monomer values (com-

pare, e.g., $\chi(^{35}\text{Cl}) = -5.64$ MHz in Na^+Cl^- [18] to the free Cl_2 value of -111.8 MHz [19].

It is possible to interpret $\chi_{aa}(\text{X})$ and estimate the fractional electronic charge δ that can be assumed to be transferred from Br to Cl when $\text{H}_2\text{S} \cdots \text{BrCl}$ is formed. In case of $\text{B} \cdots \text{Cl}_2$ complexes it has been shown that δ is given by Equation (7), where

$$\delta = \frac{\chi_{aa}(\text{Cl}_i) - \chi_{aa}(\text{Cl}_o)}{\chi_{aa}(\text{Cl}_i) + \chi_{aa}(\text{Cl}_o)} \quad (7)$$

i = inner and o = outer. In this expression for δ the effects of the angular oscillation of the BrCl subunit cancel between the numerator and denominator. It has been demonstrated [14] for complexes of the type $\text{B} \cdots \text{Cl}_2$ that $\frac{1}{2}(\chi_{aa}(\text{Cl}_i) + \chi_{aa}(\text{Cl}_o)) \approx \chi_o(\text{Cl})$, the free Cl_2 coupling constant. Hence Equation (7) can be rewritten in good approximation as Equation (8). Thus, δ is half the difference between the relative

$$\delta = \frac{\chi_{aa}(\text{Cl}_i) - \chi_o}{2\chi_o} - \frac{\chi_{aa}(\text{Cl}_o) - \chi_o}{2\chi_o} \quad (8)$$

change in χ_{aa} of the inner and outer halogen nuclei. If this also holds for a $\text{B} \cdots \text{BrCl}$ complex, the corresponding expression [Eq. (9)] is obtained. Equation (9) leads to $\delta \approx 0.05e$ for

$$\delta \approx \frac{\chi'_o(\text{Br}) - \chi_o(\text{Br})}{2\chi_o(\text{Br})} - \frac{\chi'_o(\text{Cl}) - \chi_o(\text{Cl})}{2\chi_o(\text{Cl})} \quad (9)$$

$\text{H}_2\text{S} \cdots \text{BrCl}$, which represents a small electric charge redistribution within the BrCl subunit upon complex formation and indicates a relatively weak interaction between the two subunits.

2.4 Strength of the interaction: The conclusion of a weak intermolecular interaction established in the previous section is reinforced when the intermolecular stretching force constant k_σ is considered. For an asymmetric-rotor complex $\text{B} \cdots \text{XY}$ in which the XY subunit is perpendicular to the plane of the nuclei of the planar subunit B, k_σ can be calculated from the observed spectroscopic constants by using expression (10), valid in approximation of unperturbed rigid subunits and negligible cubic

$$k_\sigma = (8\pi^2\mu/A_J) \left[B_0^3 \left(1 - \frac{B_0}{B_{\text{BrCl}}} - \frac{B_0}{B_{\text{H}_2\text{S}}} \right) + C_0^3 \left(1 - \frac{C_0}{C_{\text{BrCl}}} - \frac{C_0}{C_{\text{H}_2\text{S}}} \right) \right] \quad (10)$$

and higher force constants. [20] Here, A_J is the quartic centrifugal distortion constant appropriate to the Watson A reduction, [21] $\mu = m_{\text{H}_2\text{S}}m_{\text{BrCl}}/(m_{\text{H}_2\text{S}} + m_{\text{BrCl}})$, B_0 and C_0 are the rotational constants of the complex and $B_{\text{H}_2\text{S}}$, B_{BrCl} , etc. are the rotational constants of the monomers (see Table 6). B_0 and C_0 can be obtained separately by calculating $(B_0 - C_0)/2$ from the complex geometry of Section 2.2 and combining this with the observed $(B_0 + C_0)/2$, respectively. We have assumed that D_J determined here can be used in place of A_J . This leads to the k_σ values shown in Table 7, where the average of all observed isotopomers is $k_\sigma = 12.1(2) \text{ Nm}^{-1}$.

3. Discussion and Conclusions

The pre-reactive complex of H_2S and BrCl has been isolated and characterised by using a pulsed-nozzle Fourier-transform microwave spectrometer. The complex was found to be of C_s symmetry with the $\text{S} \cdots \text{Br}-\text{Cl}$ nuclei collinear and the H_2S in a

plane nearly perpendicular to the $\text{S} \cdots \text{Br}-\text{Cl}$ axis. The distance $\text{S} \cdots \text{Br}$ is found to be $3.094(7) \text{ \AA}$. This structure is what can be expected when the rules [4] previously enunciated for hydrogen-bonded complexes $\text{B} \cdots \text{HX}$ are applied to $\text{B} \cdots \text{XY}$. The conventional picture of the electronic structure of ground state H_2S is that the $\text{S}-\text{H}$ bonds are formed from pure $3p_x$ and $3p_y$ orbitals of S, in accord with the observed angle $\text{HSH} \approx 90^\circ$. The nonbonding electron pairs on S are then envisaged as occupying sp hybrid orbitals, each of which makes an angle of 90° with the plane of the H_2S nuclei. The observed angular geometry of $\text{H}_2\text{S} \cdots \text{BrCl}$ can then be understood if it is assumed that it is largely electrostatically determined and that the polar subunit $\delta^+\text{BrCl}^{\delta-}$ lies along the axis of one of the nonbonding electron pairs on S. There is evidence that the angular geometries of several other $\text{B} \cdots \text{BrCl}$ complexes [2] and an extended series of $\text{B} \cdots \text{Cl}_2$ complexes [11] can be rationalised on a similar basis.

Both the intermolecular stretching force constant k_σ ($=12.1(2) \text{ Nm}^{-1}$) and the intramolecular electric charge redistribution δ ($\approx 0.05e$) from Br to Cl indicate that intermolecular interaction within the complex is relatively weak. It therefore seems unlikely that a significant extent of charge transfer between H_2S and BrCl has occurred. The complex can thus be described as an "outer" type in Mulliken's language. This conclusion has also been reached for several other $\text{B} \cdots \text{BrCl}$ and $\text{B} \cdots \text{Cl}_2$ complexes, as discussed elsewhere. [1, 2]

When a series of $\text{B} \cdots \text{BrCl}$ complexes is compared with $\text{B} \cdots \text{HBr}$ it has been shown [2] that for most B's the $\text{B} \cdots \text{Br}$ distance is approximately 0.8 \AA shorter for the $\text{B} \cdots \text{BrCl}$ complexes than for the $\text{B} \cdots \text{HBr}$ complexes. A similar trend has been observed for $\text{B} \cdots \text{Cl}_2$ and $\text{B} \cdots \text{HCl}$ complexes [1] and was ascribed, in part at least, to an anisotropy in the van der Waals radius of the Cl atom. For the $\text{H}_2\text{S} \cdots \text{BrCl}$, the difference is 0.897 \AA , and is consistent with the earlier observations.

Experimental Procedure

By using a fast-mixing nozzle in our Fourier transform microwave spectrometer, complexes of H_2S and BrCl were formed, but any chemical reaction was prevented. Detailed descriptions of the fast-mixing nozzle [7] and the spectrometer [22, 23] are given elsewhere. A mixture composed of approximately 2% of H_2S (Argo International) diluted in argon was pulsed via a Series 9 (General Valve Corp.) solenoid valve from a stagnation tank at a pressure of ≈ 3 bar down the outer Teflon tube of the fast-mixing nozzle into the evacuated Fabry-Pérot cavity of the spectrometer. BrCl was flowed continuously through the inner glass capillary of the nozzle to give a pressure of $\approx 2 \times 10^{-4}$ mbar in the vacuum chamber. The complexes $\text{H}_2\text{S} \cdots \text{BrCl}$ formed at the interface of the BrCl flow and the H_2S gas pulses were observed by rotationally polarising them with microwave radiation of appropriate frequency and monitoring the subsequent spontaneous emission in the conventional manner. D_2S was made by dropping D_2O (Aldrich) onto aluminium sulfide (Aldrich) under

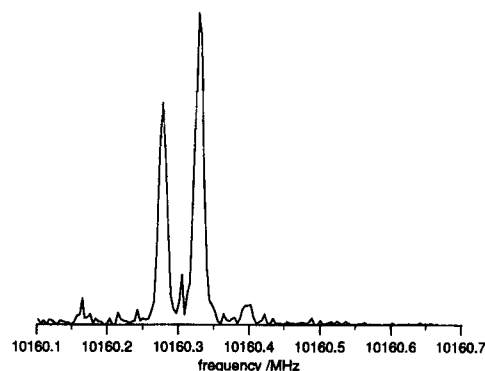


Fig. 3. Recorded frequency spectrum of two transitions in the $S_{0,5} \leftarrow 4_{0,4}$ band of $\text{D}_2\text{S} \cdots \text{BrCl}$. The assignment of J and F values can be found in Table 4. The signal is averaged over 88 gas pulses.

vacuum conditions and HDS by using a 50/50 mixture of H₂O and D₂O instead of pure D₂O. BrCl was made by mixing chlorine gas (Aldrich) with bromine vapour (Aldrich) in equal amounts. The isotopomers of complexes containing ⁷⁹Br³⁵Cl, ⁸¹Br³⁵Cl, ⁷⁹Br³⁷Cl and ⁸¹Br³⁷Cl were observed in natural abundance.

Observed transitions carried an extensive hyperfine structure arising from the presence of the electric quadrupole moments of the Br and Cl nuclei, which lead to coupling of the nuclear spin and the molecular framework angular momenta. A spectrum consisting of a few of these individual hyperfine components is shown in Figure 3. Each component has a FWHM of ≈ 15 –20 kHz, allowing frequency measurement with an accuracy of ≈ 2 kHz. The hyperfine splitting due to the deuterium nuclear quadrupole moment was too small to be resolved in species containing HDS and D₂S.

Acknowledgement: We thank the EPSRC for a research grant in support of this work.

Received: July 24, 1995 [F 173]

- [1] A. C. Legon, *Chem. Phys. Lett.* **1995**, 237, 291–298.
- [2] A. C. Legon, *J. Chem. Soc. Faraday Trans.* **1995**, 91, 1881–1883.
- [3] R. S. Mulliken, W. B. Person, *Molecular Complexes*, Wiley-Interscience, New York, **1969** and references therein.
- [4] A. C. Legon, D. J. Millen, *Faraday Discuss. Chem. Soc.* **1982**, 16, 71–87; A. C. Legon, D. J. Millen, *Chem. Soc. Rev.* **1987**, 16, 467–498.
- [5] A. J. Downs, C. J. Adams, in *Comprehensive Inorganic Chemistry* (Ed.: A. F. Trotman-Dickenson), Pergamon, Oxford, **1973**, Vol. 2, Chap. 26, p. 1107–1594.
- [6] A. C. Legon, *Chem. Soc. Rev.* **1990**, 19, 197–237.
- [7] A. C. Legon, C. A. Rego, *J. Chem. Soc. Faraday Trans.* **1990**, 86, 1915–1921.
- [8] E. J. Goodwin, A. C. Legon, *J. Chem. Soc. Faraday Trans. 2*, **1984**, 80, 51–65.
- [9] M. R. Keenan, D. B. Wozniak, W. H. Flygare, *J. Chem. Phys.* **1981**, 75, 631–640.
- [10] W. G. Read, W. H. Flygare, *J. Chem. Phys.* **1982**, 86, 2238–2246.
- [11] R. L. Cook, F. C. DeLucia, P. Helminger, *J. Mol. Struct.* **1975**, 28, 237–246.
- [12] A. C. Legon, J. C. Thorn, *Chem. Phys. Lett.* **1993**, 215, 554–560.
- [13] H. I. Bloemink, S. J. Dolling, K. Hinds, A. C. Legon, *J. Chem. Soc. Faraday Trans.* **1995**, 91, 2059–2066.
- [14] A. C. Legon, H. E. Warner, *J. Chem. Phys.* **1993**, 98, 3827–3832.
- [15] P. W. Fowler, A. C. Legon, S. A. Peebles, unpublished results.
- [16] P. Cope, D. J. Millen, A. C. Legon, *J. Chem. Soc. Faraday Trans. 2*, **1986**, 82, 1189–1196.
- [17] A. C. Legon, D. G. Lister, J. C. Thorn, *J. Chem. Soc. Faraday Trans.* **1994**, 90, 3205–3212.
- [18] F. H. de Leeuw, R. van Wachem, A. Dymanus, Symposium on Molecular Structure and Spectroscopy, Ohio, **1969**, Abstract R5.
- [19] Y. Xu, W. Jäger, I. Ozier, M. C. L. Gerry, *J. Chem. Phys.* **1993**, 98, 3726–3731.
- [20] D. J. Millen, *Can. J. Chem.* **1985**, 63, 1477–1479.
- [21] J. K. G. Watson, *J. Chem. Phys.* **1968**, 48, 4517–4524.
- [22] T. J. Balle, W. H. Flygare, *Rev. Sci. Instrum.* **1981**, 52, 33–45.
- [23] A. C. Legon, in *Atomic and Molecular Beam Methods* (Ed.: G. Scoles), Oxford University Press, Oxford, **1992**, Vol. 2, Chap. 9.